

JPL TECHNICAL PEER REVIEW EVALUATION

DYNAMICS AND CONTROL OF A 25-METER APERTURE DATE: 5/20/02

MANUSCRIPT TITLE:

VIRTUAL STRUCTURE Gossamer Telescope in GEO

JOURNAL OR SOCIETY:

AUTHOR:

ED METTLER

EXT. 4-2091

REVIEWER:

DAVID S. BAYARD

EXT. 4-8208

COMMENTS:

This paper presents an architecture and case study for a large 24 meter aperture telescope concept based on separate free-flying telescope elements orbiting in GEO. An architecture is first given for the overall end-to-end guidance and control system. The integrated dynamics, estimation and control problem is then investigated by numerical simulation using a leader-follower formation flying approach, and virtual truss control concepts. The study indicates the feasibility of the overall concept from a G&C point of view. The numerical simulation results also add realism and provide confidence building for achieving such a mission in practice. The concept appears to be relevant to JPL/NASA missions and bold new "yet-to-be-conceived" missions requiring high-resolution astrophysical imaging at optical wavelengths.

AUTHOR'S RESPONSE:

TECHNICAL REVIEWER SIGNATURE AND DATE:

David Bayard

5/20/02

JPL TECHNICAL PEER REVIEW EVALUATION

DATE: 5/20/02

MANUSCRIPT TITLE:

DYNAMICS & CONTROL OF A 25m APERTURE VIRTUAL STRUCTURE GOSAMER

TELESCOPE IN LEO

JOURNAL OR SOCIETY:

AIAA

AUTHOR: METTLER, BRECKENRIDGE, & QUADRELLI

EXT. 42071

REVIEWER: S. PLOEL

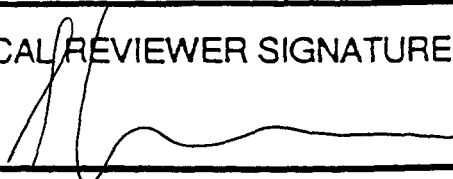
EXT. 40581

COMMENTS:

IN THIS PAPER A NOVEL ARCHITECTURE IS PRESENTED TO MODEL/
ANALYZE / CONTROL AN ORBITING VIRTUAL STRUCTURE GOSAMER
TELESCOPE. THE AUTITORS PROVIDE A STATE OF THE ART
DEVELOPMANT USING THE IDEA OF A "VIRTUAL TRUSS". THIS IS
A WELL WRITTEN PAPER THAT PROVIDES VALUABLE CONTRIBUTIONS
TO THIS EXCITING FIELD.

AUTHOR'S RESPONSE:

TECHNICAL REVIEWER SIGNATURE AND DATE:



5/20/02

DYNAMICS AND CONTROL OF A 25-METER APERTURE VIRTUAL STRUCTURE GOSSAMER TELESCOPE IN GEO*

Edward Mettler, William G. Breckenridge, and Marco Quadrelli
Jet Propulsion Laboratory, California Institute of Technology
4800 Oak Grove Drive, Pasadena, CA 91109-8099
E-mail: Edward.Mettler@jpl.nasa.gov

Abstract

In this paper we conduct a feasibility analysis of a 25-meter aperture virtual-structure space telescope example concept based on formation control of separated free-flying optical modules orbiting the Earth at GEO. We develop a Formation Flying implementation approach, and design and analyze the dynamics, control, metrology and estimation methods. The geostationary telescope (GEOTEL) (**Figure 1**) is composed of 6 bodies: Primary Mirror Membrane, Free Flying Mirror, Focal Plane Assembly (with secondary & tertiary stages), Primary Figure Sensor, Scanning Electron Beam for Primary shape adjustment, and Orbiting Sunshade. The reflective optics telescope [1] under consideration represents an advanced gossamer concept that can have many variations, extending to concepts employing large diffractive membrane primaries (**Figure 11**). Applications of such concepts are envisioned in the areas of astrophysical direct exo-solar planet imaging in optical wavelengths, as well as for super-precision Earth observation (**Figure 10**).

The paper describes the formation flying system modeling in the GEO environment and its simulation during a retargeting maneuver under proportional thruster control. We define a gossamer space telescope formation as an ensemble of orbiting optical modules acting as one virtual-structure telescope system. After the formation is in place, one may identify what is known as the virtual-truss, i.e. the connection between the elements of the formation that provides configuration spatial rigidity based on the information and control flow between them. The dynamics model takes into account the orbital and 3D dynamics of each module. The formation estimator provides estimates of the inter-module relative position and velocity vectors,

given the measurements of a distributed Radio Frequency (RF) Metrology system and a centralized Optical Metrology module. The optic module's state measurements are provided by models of star trackers, gyros, and accelerometers, together with their bias and noise models. The individual module actuation systems consists of proportional micro-Newton level Field Emission Electrostatic thrusters (FEET's) for precision station-keeping, as well as Newton level thrusters used for retargeting the entire formation. The control system design consists of a proportional-derivative feedback plus acceleration feed-forward. This ensures that modeling errors are compensated appropriately, and that the commanded slew is tracked accurately. Key findings support the feasibility of Formation Flying to enable virtual-structure gossamer Space Telescopes.

Keywords: Formation flying, autonomous control, virtual structure, gossamer telescope.

Introduction

In this paper a concept definition and feasibility analysis are developed for the Formation Flying of a 25-meter aperture space telescope based on control of separated free-flying optical modules orbiting the Earth at GEO. The geostationary telescope (GEOTEL) (**Figure 1**.) is composed of 6 bodies: Primary Mirror Membrane, Free Flying Mirror, Focal Plane Assembly (with secondary & tertiary stages), Primary Figure Sensor, Scanning Electron Beam for Primary shape adjustment, and Orbiting Sunshade. The reflective optics telescope under consideration [1] represents an advanced gossamer concept that can have many variations, extending to concepts employing large diffractive membrane primaries (**Figure 11**).

* Copyright © 2002 by the American Institute of Aeronautics and Astronautics, Inc. The U.S. Government has a royalty-free license to exercise all rights under the copyright claimed herein for Governmental purposes. All other rights are reserved by the copyright owner.

The overarching goal of this study is to assess the basic technical feasibility of implementing an Earth imaging 25-meter GEO telescope by maneuvering and stationkeeping the separate optical modules in the required geometric configuration and precision that obviates the need for a connective metering structure (Figure 10).

The formation flying definition includes:

- Centralized relative optical sensing
- Decentralized relative RF sensing and absolute celestial-inertial guidance
- Centralized formation state estimation and optical model positioning prediction
- Telescope Commanding methodology from acquisition to precision targeting and re-pointing
- Telescope element(s) positioning error allocations
- Analysis of metrology system performance and error sensitivities
- Assessed formation control capability
- Free-flying elements orbital characteristics and dynamics analysis
- Targeting methodology and imaging scenario analysis
- Primary mirror shape sensing and formation vector metrology

An example from numerical simulation of an imaging scenario in geostationary Earth orbit closes the paper.

GEOTEL Formation Control Concept

A candidate GEOTEL formation concept is shown in Figure 1. GEOTEL is composed of 6 bodies: A 25-meter Primary Mirror Membrane (PMM), Free Flying Relay Mirror (FFM), Focal Plane Assembly (FPA with a Fast Steering Mirror (FSM) and secondary/tertiary stages), Primary Figure Sensor (PFS), Scanning Electron Beam (SEB) for Primary shape adjustment, and Orbiting Sunshade (OSS). The off-axis reflective optics telescope under consideration represents an advanced gossamer concept that can have many variations, extending to concepts employing a very large diffractive membrane primary. (Figure 11). A distributed sensing and control approach enables a virtual-truss 3D rigidity of the separated telescope elements and maintains the tight tolerances on overall planarity and alignments of the optical system. Relative measurements between linear neighbors and an off-axis observer are depicted. Range, range rate, azimuth and elevation data are obtained and processed both locally on each body and globally by a 'Commander' function, which serves as the formation Navigator and the Command, Control, and Communications Executive. This distribution of sensing, decision, and control action at the Element Level and the Formation Executive Level optimizes the division of autonomous management functions for

the formation. The challenges in formation sensing and control are:

- 1) The 25-meter, $f/10$, Primary Mirror membrane and its necessary optical path alignments place severe constraints on multi-body metrology and stationkeeping precision for targeting and imaging (sub-micron and sub-arcsecond knowledge of individual range and bearing measurements, and sub-mm real-time motion control);
- 2) Diffraction limited imaging drives the requirement for the ultra-fine placement of the target image in the entrance aperture of the Focal Plane Assembly to enable focal plane image stabilization and wave-front correction; and
- 3) The need for coordinated multi-body placement initialization, line-of-sight pointing maneuvers, and targeting strongly motivates the Formation Control autonomy concept
 - to be based on real-time guidance utilizing an onboard analytical model of the telescope optical system,
 - to employ both centralized and decentralized sensing and metrology, and multi-level control authority (in a formation executive function, and in the individual free-flying modules).

The Formation Metrology and Control System overall performance objectives are:

- To initialize the image formation process using Open loop Predictive Control to place the target image within the entrance aperture of the focal Assembly with an accuracy that enables an image sensed vernier centering and stabilization stage to function
- To respond in a closed loop mode to focal plane image tracking offset correction signals that may be generated by the vernier stage on the Focal Assembly
- To reorient the separated formation ensemble as a unit to slowly repoint the telescope field of view for new-theatre imaging operations
- To control the Free-Flying (relay) Mirror positioning and attitude for agile in-theatre targeting

The following operational assumptions and constraints have been made for the system:

- The system has already undergone deployment and acquisition such that all elements are at their nominal orbital positions, accurate to several cm.
- The PMM is stationkept so that its CG follows a geostationary orbit, and the CG of the PMM is located at its mechanical center.
- The optical system is assumed to have been calibrated using a ground beacon reference, in

concert with 6-dof (degrees-of-freedom) ray path mapping procedures (FFM and FSM), resulting in on-board system optical models which are accurate enough to predict the principle ray direction and target image location in support of routine FFM and FSM positioning operations.

- The OSS is both attitude and orbit controlled to provide shade of the PMM over the entire year.

The telescope Formation Control requirements and assumptions are described next: All elements of the formation stationkeep (hold relative position) with respect to the Primary Mirror. Relative position knowledge is provided by an RF/Optical metrology system. Absolute orbit position and attitude is provided by the Global Differential GPS and Inertial Navigation subsystems. Because of the large dynamic range between acquisition, targeting maneuvers, and imaging, the metrology system is multi-stage (e.g., coarse-RF, fine-Optical). Requirements on the accuracy and stability of the attitude and position knowledge and control are derived from the on-orbit process of configuring and using the telescope in which **Predictive Open Loop** image acquisition is followed by **Closed loop** focal plane image sensed correction of offset and image stabilization. All translational and rotational control to required accuracies is done using micro-thrusters and small reaction wheels.

The Telescope axis is defined as the line perpendicular to the ring of the Primary Mirror and is pointed in the desired inertial direction by attitude control of the Primary (2 dof).

- The shape of the mirror surface is to be known/controlled, e.g. to be spherical with specified radius of curvature (500m) and center of curvature on the telescope axis.
- The shape is measured by the Figure Sensor.
 - The Figure Sensor must stationkeep with respect to the Primary at/near the desired center of curvature.
 - The Figure Sensor must know/control its attitude to be aligned with respect to the Primary (3 dof).
 - The Figure Sensor must measure the shape of the mirror surface.
- The shape actuator is the Electron- Beam (E-Beam):
 - The E-Beam must stationkeep with respect to the Primary at/near an on-axis point behind the Primary (e.g. 50m).
 - The E-Beam must know/control its attitude to be aligned with respect to the Primary (3 dof).

- The E-Beam will irradiate the electrostatic membrane mirror to correct errors in the shape.
- The final shape of the Primary is measured and used by the optical model

The telescope steering must specify the desired telescope inertial LOS, within a limited range of the telescope axis. The Primary provides knowledge of its attitude. The Primary shape is provided by the Figure Sensor and data is sent to the **Optical Model**. The optical model will determine the required focal point with respect to the Primary (3 position. and 2 attitude. dof). For any Theater, the Primary Mirror and Focal Plane Assembly remain stationary and the Free Flying Mirror moves around in the 3.5m square theater image (500km at the surface) to intercept various individual target images (17.5mm square, 2.5km at the surface).

Error allocations associated with the Target Image Centered within the FPA Entrance Aperture result in: ± 10 mm per axis lateral (2 dof) and ± 10 mm on-axis, for depth of field assumption. Further suballocation in Image Location Errors include both knowledge and control contributions combined on an RSS basis: FPA Image Location Error (3.54 mm); FFM Image Location Error (3.54 mm); Optical Model Image location Error (8.66 mm).

Allocations in the Closed Loop Focal Plane Image Sensed Stabilization Mode resulted in an implementation using a 2-axis fast steering mirror (FSM) on a piezo-translator stage (PZT) to control the final lateral and on-axis Centering Corrections of the Target Image in the FPA. This focal plane image stabilization control must provide < 500 microns lateral centering and on-axis errors in order to be within the dynamic range of a Liquid Crystal Wavefront Corrector stage. It must also provide high bandwidth ($>> 20$ Hz) image stabilization for near diffraction limited resolution, and sensing of "excessive offset" for the Predictive Mode Control.

GEOTEL Formation Dynamics

The GEOTEL formation's most basic active elements are 5 free-flying optical modules. The free flyers are:

- S0, the primary mirror membrane (PMM)
- S1, the free flying mirror (FFM)
- S2, the Focal Plane Assembly (FPA)
- S3, The Primary Figure Sensor (PFS)
- S4, the Scanning Electron Beam (SEB)

With S_0 at the origin of the coordinate frame defined by the axes (T, C, N), (**Figure 3**) the relative coordinates of S_i , $i=1, \dots, 4$ are

Table 1. GEOTEL Coordinates.

S_1	$p_1 = 40$	$q_1 = 0$	$r_1 = 235.7753$
S_2	$p_2 = 50$	$q_2 = 0$	$r_2 = 240$
S_3	$p_3 = 0$	$q_3 = 0$	$r_3 = 500$
S_4	$p_4 = 50$	$q_4 = 0$	$r_4 = -50$

Where (p_i, q_i, r_i) are the formation coordinates of the S_i . The coordinates above define a virtual formation that is to be maintained throughout the flight. Referring to **Figure 2**, the following assumptions are used in this paper:

- The formation is composed of five rigid bodies (sunshade dynamics is neglected).
- The orbit is circular.
- The formation dynamics is described (and numerically integrated) with respect to the Orbiting Reference Frame, to be described next.

The motion of the system is described with respect to a local vertical-local horizontal (LV-LH) orbiting reference frame $(x,y,z)=F_{ORF}$ of origin O_{ORF} which rotates with mean motion Ω and orbital radius R_0 . A general type of orbit can be accommodated in the model, as the orbital geometry at the initial time is defined in terms of its six orbital elements, and the orbital dynamics equation for point O_{ORF} is propagated forward in time under the influence of the gravitational field of the primary (Earth for LEO, Sun for Deep Space applications) and of the Earth as a third body perturbation effect.

The origin of this frame coincides with the initial position of the center of mass of the system, and the coordinate axes are z along the local vertical, x toward the flight direction, and y in the orbit normal direction. The inertial reference frame $(X,Y,Z)=F_I$ is geocentric inertial for LEO (X points toward the vernal equinox, Z toward the North Pole, and Y completes the right handed reference frame), and heliocentric inertial for other applications.

The orbit of the origin of F_{ORF} is defined by the six orbital elements a (semimajor axis), e (eccentricity), i (inclination), Ω_L (longitude of ascending node), ω (argument of perigee), ν (true anomaly), and time of passage through perigee.

From **Figure 2**, the position vector of a generic structural point with respect to O_{ORF} is denoted by ρ_i , and we have $r_i=R_0+\rho_i$. We define the state vector as $X=(R_0, V_0, \rho_1, q_1, v_1, \omega_1, \dots, \rho_5, q_5, v_5, \omega_5)^T$, where q_i and ω_i represent the quaternion and angular velocity vector of the i -th spacecraft with respect to F_I .

Assume that the several modules can be modeled as rigid bodies, that is, no flexible structural modes are present. Assume further that the translational dynamics and the rotational dynamics are uncoupled. The kinematics equations are as follows:

$$\begin{aligned} v_i &= \dot{\rho}_i \\ \omega_i &= \Gamma(q_i) \dot{q}_i \\ \omega_w &= \dot{\theta}_w \end{aligned}$$

The **translational** dynamics equations are:

$$\begin{aligned} \ddot{\rho}_i &= -\ddot{R}_0 - \Omega \times \Omega \times \rho_i - 2\Omega \times \dot{\rho}_i + \frac{R\ddot{r}_i}{m_i} \\ \ddot{r}_i &= \left(\frac{f_s}{m_i} - \mu_s \right) \frac{r_i}{|r_i|^3} - \mu_E \frac{(r_i - r_E)}{|r_i - r_E|^3} + A_i \frac{f_a}{m_i} \end{aligned}$$

Where: ρ_i = relative position vector of body i wrt. ORF, A_i = rotation matrix of i -th body frame wrt. inertial, R_0 = orbital radius vector to origin of ORF, Ω = orbital rate, R = rotation matrix of ORF to inertial frame, f_s = magnitude of solar force, μ_s = solar gravitational parameter, μ_E = Earth gravitational parameter $= 3.986005 \times 10^{14} \text{ m}^3/\text{s}^2$, f_a = actuator force, m_i = module mass with wheels added.

The **rotational** dynamics equations are:

$$\begin{aligned} J_i \dot{\omega}_i + \dot{h}_i + \omega_i \times (J_i \omega_i + h_i) &= r_{cp2cm} \times f_s \frac{r_i}{|r_i|^3} + \tau_a \\ \dot{h}_i &= -\tau_w \end{aligned}$$

Where ω_i = body angular rate, f_s = magnitude of solar force, τ_a = actuator torque, τ_w = wheel input torque, J_i = spacecraft moment of inertia, h_i = angular momentum of wheels, r_{cp2cm} = vector from center of mass to center of pressure of body i . **Figure 3** (left) depicts the bird-eye view of looking down at the C-axis. S_0 is allowed to translate freely along the T, C, and N axes, and also to sway about the C-axis, which induces an anti-clockwise rotation θ_y .

In order to maintain the same relative position of the GEOTEL formation, each free flyer S_i therefore has to move along with the translational motion of S_0 , and also to translate from the solid circular position to the dotted position as shown in **Figure 3** to compensate for the angular rotational of S_0 . Note that in the figure L_i is the projection of the line joining S_0 and S_i on the (TN)-plane; S_0 and S_i may actually have different coordinates in the C-axis.

Control Model

The translation control actually implemented on the i -th optics module is of the form

$\mathbf{f}_i = \mathbf{K}_p^i(\mathbf{q}_{Cmd}^i - \mathbf{q}_{Est}^i) + \mathbf{K}_v^i(\mathbf{v}_{Cmd}^i - \mathbf{v}_{Est}^i) + \mathbf{M}^i \mathbf{a}_{Cmd}^i$ where \mathbf{K}_p^i and \mathbf{K}_v^i are translation control gain matrices, \mathbf{M}^i is the module mass matrix, \mathbf{q}_{Est}^i and \mathbf{q}_{Cmd}^i represent the estimated and commanded translation state, respectively.

The rotational control is of the form

$\boldsymbol{\tau}_i = \boldsymbol{\Gamma}_p^i(\boldsymbol{\lambda}(\theta_{err})_{Cmd}^i - \boldsymbol{\lambda}(\theta_{err})_{Est}^i) + \boldsymbol{\Gamma}_v^i(\boldsymbol{\omega}_{Cmd}^i - \boldsymbol{\omega}_{Est}^i) + \mathbf{J}^i \boldsymbol{\alpha}_{Cmd}^i$ where $\boldsymbol{\Gamma}_p^i$ and $\boldsymbol{\Gamma}_v^i$ are rotational control gain matrices, \mathbf{J}^i is the module moment of inertia matrix, $\boldsymbol{\lambda}$ is the eigenaxis of rotation, θ_{err} is the magnitude of rotation corresponding to the difference between the commanded and the estimated quaternions, and $\boldsymbol{\omega}$ and $\boldsymbol{\alpha}$ are the angular velocity and acceleration respectively.

One of the control objectives is to minimize the errors from the Primary Membrane described as follows (see Figure 3-left):

$$\begin{aligned}\epsilon_x &= x_i - x_0 - L_i \sin(\theta_y(t) + \theta_i) \\ \epsilon_y &= y_i - y_0 - q_i \\ \epsilon_z &= z_i - z_0 - L_i \cos(\theta_y(t) + \theta_i)\end{aligned}$$

Where $L_i = \sqrt{p_i^2 + r_i^2}$ and $\tan(\theta_i) = p_i/r_i$. The variables x_i , y_i , and z_i denote the position coordinate of S_i along the T-, C- and N-axis, respectively. We assume here that the free flyer body coordinate axes are aligned exactly with T, C, and N at the initial time. **Figure 3** (right) shows the command profile and its time derivative adopted for the present study. The profile is a function of time of $f(t) = (3t^2T - 2t^3)/T^3$ varying from 0 at $t = 0$ to a normalized value of 1 at $t = T$.

Formation Optical Metrology

The proposed GEOTEL optical metrology is a novel system that enables determination of range, bearing, and orientation of all formation system elements along with the figure of the Primary Mirror. The underlying vector metrology is based on the following concepts:

- **Array Heterodyne Interferometer (AHI)** The Array Heterodyne Interferometer (AHI) is a heterodyne interferometer that simultaneously measures relative range of multiple targets on a surface and enables multi-target high precision linear and angular metrology [1], **Figure 6**. The target surface is illuminated with a beam of light which is reflected and then interfered with a

reference wavefront. The resulting interference pattern is detected with an array of detectors, for example a CCD or an APS (Active Pixel Sensor). Because it is a heterodyne interferometer, i.e. target and reference beams are shifted in frequency relative to each other by a heterodyne frequency, each detector, or CCD pixel, produces an AC output oscillating at the heterodyne frequency. The phase of this oscillation, relative to a reference oscillator or another pixel, is proportional to the relative range.

- **Modulation Sideband Technology for Absolute Ranging (MSTAR)**

MSTAR enables unambiguous range determination for moving targets. The MSTAR sensor is an upgrade to a heterodyne interferometer that turns it into a range sensor with a long ambiguity range, while retaining high precision of a heterodyne interferometer and its simple signal processing. MSTAR technology provides the following benefits, which make it a breakthrough technology for future separated spacecraft applications. First, it is a two-color interferometer implemented with a *single* frequency stable laser, a key consideration for long-range metrology, because laser frequency stability becomes a serious issue. Use of single frequency stationary and stable laser greatly mitigates frequency stability issues. Second, measurements at two wavelengths are simultaneous, which enables measurements of non-stationary targets, a must for formation flyers. Third, two wavelengths are generated and isolated by a combination of high-speed phase modulators and frequency shifters. The high-speed phase modulators are currently available as integrated optics components and the next generation of polymer-based phase modulators is being developed which will enable hybrid integration of the sensor into a small rugged package. Fourth, no high-speed signals need to be detected at the photo-detector providing simple signal processing and high sensitivity, because detectors can be slow.

- **Boresight Pointing Sensor (BPS)**

The BPS allows precision sensing of pointing optics and enables high-precision angular metrology without high-precision pointing optics. The addition of MSTAR and BPS to the Array Heterodyne Interferometer (AHI) turns the AHI from purely a static figure sensor into a full formation metrology sensor. A GEOTEL optical metrology sensor configuration using MSTAR and AHI is shown in **Figures 1, 6**. The sensor, located

at the center of curvature of the Primary Mirror, illuminates the scene containing all the formation flying elements. The returning light from the Primary Mirror and retro-reflective targets mounted on the system elements is imaged on the APS. The phases of heterodyne modulations at each corresponding pixel on the APS are on-board processed to give range, and the image centroids are calculated on the chip to give the bearing angle of the target corresponding to a given spot.

The above innovations and technologies enabled us to combine Primary Mirror figure sensor and formation optical metrology into a single package located on one element of the formation. This results in significant savings in terms of cost, weight and complexity of hardware and, because only retroreflective patches need to be mounted on other elements, makes the system uniquely suited to lightweight flexible structures.

RF Metrology (AFF) Model

The RF metrology (AFF) subsystem collects from each formation element receiver data of range and phase, at each of 3 antennae, of signals from a transmitter on each other element. There are 6 one-way links for each element pair. The 6 links provide an RF “truss” to determine the relative position and attitude of the two elements. Assuming that all the common errors in the system have been calibrated (or solved for) and attitude is known accurately from Attitude Estimation, each “truss” can be viewed as an independent measurement of the relative position of the two elements. Previous analysis has shown that the measurement accuracy can be characterized by independent range (along the LOS) and bearing (2 dof pointing normal to the LOS) errors. Simulation of the AFF subsystem can be carried out on two levels, simulating individual RF links as input to an extensive processing algorithm or simulating the outputs of the process, the equivalent “truss” measurements. The latter is more suitable for a higher-level system functional simulation where the subsystem low-level detail is not important.

We call *perfect measurement* the vector difference of the “true” positions of two elements of the formation, as defined by the simulation dynamics, and mapped to the coordinate system used by the Formation Estimator. Conversely, we call *simulated output measurement* the perfect measurement plus an error vector randomly generated from the population represented by the measurement covariance matrix that is also an output of this simulator. Previous analyses of the performance of the AFF estimate of the range and bearing between two formation elements has provided the following simplified approximations to the

estimation accuracy. The assumptions of the sensor model are as follows. First, the attitude estimate accuracy is small with respect to required bearing accuracy. Second, the alignment between AFF and attitude sensors is well calibrated. Third, the AFF antenna locations with respect to normal telecom are well calibrated. Fourth, the AFF clock differences are well calibrated. Fifth, the AFF phase difference biases are well calibrated. AFF usually puts a large margin on this due to other noise, e.g. multipath. Observations are 6 ranges and 4 phase differences. The phase differences enhance bearing accuracy but not range. The accuracy of an estimate from one set of AFF measurements is approximately $v_{\text{range}} = v_r / 6$ and $v_{\text{bearing}} = v_{\text{ph}} * 2 / (d_i^2 + d_j^2)$ per axis, for the measurement from body-i to body-j, where d is a metric of the AFF receiver array size [meters] and may vary by element, v_r is the variance of range measurements from the ranging code correlation $\approx (1\text{cm})^2$, v_{ph} is the variance of phase measurements from carrier correlation $(10\mu\text{m})^2$.

Formation Commander

A functional diagram of the Formation Commander is shown in **Figure 7**. The formation of telescope elements is considered as a single “rigid body” with a telescope Line-of-Sight fixed in “body” coordinates. That coordinate system is defined co-linear with the PMM coordinate system. All elements have fixed locations with respect to the Primary Mirror except the Free Flying Mirror that is at its mean position. The desired formation attitude places the body-fixed LOS in the inertial direction of the desired Target. This only defines two degrees of freedom. The third dof, rotation around the LOS, can be used to satisfy some other constraint, e.g. sun direction on un-shaded elements. If the third dof is used to minimize the formation rotation, the required formation rotation to retarget is defined by current LOS unit-vector cross Target unit-vector. The turn axis is the direction of the cross-product vector, and the turn angle is arcsine of the magnitude of the cross-product. The formation configuration with the FPA offset from the PMM axis is used to keep the telescope LOS away from the formation elements to avoid obscuration and stray light.

The Free Flying Mirror is intended to intercept a target image from the Primary Mirror and precisely reflect/redirect it into the entrance aperture of the Focal Plane Assembly. To accomplish this, two conditions must be met at the FFM position. The first one is that FFM must be on the line from the PMM to the Image. The second one is that the PMM-FFM-FPA path length must equal the focal length of the telescope.

A solution puts the FFM on an ellipsoid, with foci at the FPA and PMM, at the intersection with the PMM-

Image line. Alternatively, the FFM is at the intersection of the PMM-Image line and the plane bisecting the FPA-Image line segment as shown in **Figure 8** at the left. The mirror normal is oriented to bisect the lines to the FPA and PMM. For small changes in target location w/n a field around the formation aim-point, the FFM can be moved to intercept nearby image points as shown in **Figure 8** at the right.

Formation Estimator

A functional diagram of the Formation State Estimator is shown in **Figure 9**. An estimator of the formation relative state is needed both in simulations as well as in real life because the control of the formation rigidity demands an accurate knowledge of the relative range and range rate between adjacent spacecraft. In this section, for simplification, we deal with the relative translation estimator based only on the AFF radio-frequency metrology (**Figure 5**). The current implementation of the translation estimator estimates only the relative position and velocity of adjacent spacecraft. This implies that the measurements used depend only on relative position and are not correlated to other system variables such as the attitude estimates of the spacecraft, or the misalignments between various subsystems. This assumption is acceptable only as long as the effects of these secondary disturbances are small compared to the errors in the relative position measurements (e.g. attitude estimate error is much less than metrology bearing measurement uncertainty). The metrology measurements are also assumed to be independent and uncorrelated between measurements, which implies that any common factor within the metrology subsystem have been removed, by calibration or estimation, in the internal processing. The radio-frequency metrology AFF subsystem collects from each formation element receiver data of range and phase, at each of three antennae, of signals from a transmitter to three receivers on each element. This represents six one-way links for each element pair. These six links provide an RF "truss" to determine the relative position and attitude of the two elements. Assuming that all the common errors in the system have been calibrated (or solved for) and attitude is known accurately from Attitude Estimation, each "truss" can be viewed as an independent measurement of the relative position of the two elements. Previous analysis has shown that the measurement accuracy can be characterized by independent range (along the line of sight) and bearing (2 dof) pointing normal to the line of sight) errors. Simulation of the AFF subsystem can be carried out on two levels, simulating individual RF links as input to an extensive processing algorithm or simulating the outputs of the process, the equivalent

"truss" measurements. The latter is more suitable for a higher-level system functional simulation where the subsystem low-level detail is not important. The perfect measurement is the vector difference of the "true" positions of the two elements of the formation, as defined by the simulation dynamics, and mapped to the coordinate system used by the Formation Estimator (if different than that used by the dynamics). The simulated output measurement vector is the perfect measurement plus an error vector randomly generated from the population represented by the measurement covariance matrix that is also an output.

After measurement and estimation, the following input data is available to the Commander/Controller of the formation. For each module, we have: linear position, velocity, acceleration vectors, quaternion, angular velocity, angular acceleration vectors in relative bearing and bearing rate, relative range and range rate, all measured with respect to the vehicle's body frame, the neighbor spacecraft body frame, and the inertial frame. The estimation of the attitude of each module is decentralized. Star tracker and gyro measurements are each spacecraft are processed to give the modules attitude relative to an inertial frame. Accelerometer and relative position measurements in the form of an AFF sensor are also available.

The measurement covariance matrix, \mathbf{R} , is characterized by range and bearing (2dof) estimate uncertainties and has its principal axes aligned with the measurement vector. Let the vector $\mathbf{v} = r\mathbf{u}$ where r is the range and \mathbf{u} is the unit vector along the LOS, v_r the variance of range estimate $= \sigma_r^2$, and v_b the variance of bearing estimate, per axis $= \sigma_b^2$. Then the measurement covariance matrix is $\mathbf{R} = v_r \mathbf{u}\mathbf{u}^T + v_b r^2(1 - \mathbf{u}\mathbf{u}^T)$. A random vector from the population represented by \mathbf{R} can be generated from independent, zero mean, unit variance random numbers, w_i , by $\mu_{\text{error}} = \sigma_r \mathbf{u} w_1 + (1 - \mathbf{u}\mathbf{u}^T)$. The estimator structure is as follows:

$$\begin{aligned} \mathbf{r} &= \mathbf{y} - \mathbf{H}\mathbf{x} \\ \mathbf{K} &= \mathbf{X}\mathbf{H}^T(\mathbf{H}\mathbf{X}\mathbf{H}^T + \mathbf{R})^{-1} \\ \mathbf{x}_+ &= \mathbf{x} + \mathbf{K}\mathbf{r} \\ \mathbf{X}_+ &= (\mathbf{I} - \mathbf{K}\mathbf{H})\mathbf{X}(\mathbf{I} - \mathbf{K}\mathbf{H})^T + \mathbf{K}\mathbf{R}\mathbf{K}^T \end{aligned}$$

Where \mathbf{r} is the measurement residual, \mathbf{K} is the extended Kalman filter gain, \mathbf{X} is the estimator state covariance, \mathbf{x} the estimator state, and the subscripts + (-) denote the state before or after update. Optical metrology measurements can be treated in the same way as the RF metrology described above, and combined to give even higher precision state estimates. Consider the estimation of the relative position of two separated spacecraft in a geocentric orbit. Accelerometer and relative position measurements in the form of an AFF sensor are available. The relative acceleration in inertial coordinates between the center

of mass of spacecraft 0 and spacecraft 1 is given by $\mathbf{a}_i = \mathbf{u}_i/m_i - \mathbf{u}_0/m_0 + \mathbf{w}_i$, where m_0 and m_i are the masses of the two spacecraft and \mathbf{u}_0 and \mathbf{u}_i are the applied forces to each of the spacecraft which derive from sources such as thrusters, solar pressure, and gravity effects, and \mathbf{w} represents kinematics terms perturbing the dynamical equation. The accelerometer measurements for one spacecraft are given in the accelerometer body frame, and their sensor model includes accelerometer bias and measurement noise. The last equation can be used to propagate the relative state measurement in the estimator.

This simplified form of the translation estimator contains only the relative (to the Primary Mirror) position and velocity vectors of the formation in an inertially fixed Reference Coordinate system. The measurements used to estimate the relative position also depend on other state variables that were assumed to be known well enough that their exclusion did not significantly change the position estimation. If those assumptions are not valid then those other states should be included in the estimator, significantly increasing the number of states to be estimated. Other state variables that might be included in the estimator are: Relative external/disturbance accelerations (e.g. due to solar pressure); Accelerometer bias, alignment and scale factor; Attitude of all the elements of the formation; Attitude, rate, external/disturbance angular accelerations; Gyro bias, alignment and scale factor; Location/alignment errors of all sensors within each element; Star tracker, AFF antenna array, Optical Metrology components; AFF system internal systematic errors (Relative clock offsets, Differential phase measurement biases, multipath biases); and Optical Metrology internal systematic errors.

Those states that can be considered constant for a long duration can be solved for in a periodic system calibration with a separate, special purpose, estimator calibration. These estimates of invariant states would be used as parameters in the estimator to estimate the dynamic states during the observation period. Such calibrations usually require a series of maneuvers to make the states observable, but complete observability may still not be possible. Multiple states that cannot be distinguished while in/near the desired formation configuration should be represented by a subset that has the same net effect as the complete set and are distinguishable. Estimating too many, highly correlated states results in a large and poorly conditioned covariance matrix and the numerical difficulties may be caused. The selection of which states to solve for is the "art" part of estimator design. Separating these correlated errors is usually possible with large changes in the relative range and bearing between the two elements, but when mapped back to net effect at the

observing configuration there is usually little improvement.

Numerical Simulation

The simulation architecture is shown in **Figure 4**. and **Figure 12** depicts the FFM position error in meters vs. time during a 1 degree retargeting in the orbital plane. Relative positioning accuracies of the optical modules during retargeting are sufficient to maintain the optical ray path and placement in the FPA entrance aperture. Stationkeeping and target image placement precision during target observation using proportional field emission micro-thrusters (FEEP's), and based on the combined AFF and Optical Vector Metrology, is predicted to be in the range of 100 to 300 microns and sub-arcsecond orientation. This will place the target image within the desired 500 microns dynamic range constraint of the wavefront corrector in the FPA.

Key Findings

1. The Telescope off-axis configuration with FPA, E-Beam, Primary Mirror, Relay Mirror, Primary Figure Sensor, and Sunshade has adequate geometric properties for formation observability without an added off-axis observer platform (**Figure 1**)
 - Center of Primary Mirror is nominally 50-meters from the local vertical axis
 - Figure Sensor free-flyer at primary mirror center of curvature also serves as the platform for formation Optical Vector Metrology
 - Development of a common Figure and Vector Metrology Sensor is feasible
 - Precision Optical Vector Metrology can simultaneously observe range and bearings of Primary Mirror, Free-flying Mirror, and Focal Plane Assembly from its location on the Figure Sensor platform
 - Duplex links of Differential GPS Ka-band Transceivers and Patch Antennas on each element provide robust coarse relative range, range rate, and bearing for formation nominal acquisition and collision avoidance
2. Formation Control using MEMS micro-N to milli-Newton proportional FEEP's (field emission electrostatic propulsion) should be capable of supporting stationkeeping precision and bandwidth required to place the target image within 3 to 4 mm of the center of the Focal Assembly entrance aperture
3. Although it may not be needed, a Focal Plane Assembly Fast Steering Mirror responsive to any "jitter" error signals from the focal plane will

ensure stabilization of the image for near diffraction limited resolution.

Conclusions

In this paper we have investigated the dynamics, control, and estimation feasibility for a formation flying space telescope composed of 6 bodies: Primary Mirror Membrane, Free Flying Mirror, Focal Plane Assembly, Primary Figure Sensor, Scanning Electron Beam, and the Orbiting Sunshade. Applications of such concepts are envisioned in the areas of astrophysical imaging in optical wavelengths, as well as precision Earth observation. The analysis included dynamics modeling in the GEO environment, formation flying estimation, and control design with metrology and actuator models. We have ascertained the formation control feasibility of the desired performance of the system in stationkeeping and during a retargeting maneuver that was demonstrated by numerical simulation.

Advanced Formation Flying metrology, estimation, and control technology is enabling for all virtual structure gossamer space telescope concepts. The general feasibility of formation flying the telescope's separated optical elements is based on new metrology and control architectures, implementation innovations, and our near term performance projections for these technologies.

A practical (realistic funding profile and prototype developments) time horizon of technology readiness for space flight demonstration of the identified methods and implementations described herein is within ten years from the current art. This is a conservative forecast and is grounded in the foundation of precursor research and development now taking place in many government and industry laboratories in the U.S. and Europe. The impact of Formation Flying large aperture lightweight telescopes on Earth remote sensing and astrophysics will be revolutionary, and make possible first-order observability breakthroughs at an affordable investment of national resources.

Acknowledgements

The research of the authors was carried out at the Jet Propulsion Laboratory, California Institute of Technology, under a contract with the National Aeronautic and Space Administration.

We gratefully acknowledge the expertise and contributions of our colleagues Drs. David S. Bayard and Serge Dubovitsky. We also wish to thank our JPL sponsor Dr. Fred Y. Hadaegh for his valued advice and support. Our sincere appreciation also goes to Dr. Ivan Bekey, President of Bekey Designs, Inc; and Dr. Richard Baron of JPL for their basic gossamer telescope concepts.

References

- [1] Mettler, E., Bayard, D., Breckenridge, W., Dubovitsky, S., Quadrelli, M.: *Precision Formation Flying Concept Definition for a 25-meter Aperture Earth Imaging GEO Telescope*. JPL Report D-20128. January 26, 2001.
- [2] Hadaegh, F. Singh, G. Quadrelli M, and Shields, J.: *Modeling and Control of Formation Flying Spacecraft in Deep Space and Earth Orbits*, Terrestrial Planet Finder Technology Interchange Symposium, April 27, 2000.
- [3] Quadrelli M., Hadaegh, F.Y., Singh, G., and Shields, J.F.: *Some observations on the Dynamics and Control of Spacecraft Formations*, presented at the IFAC Conference on Aerospace Controls, Bologna, Italy, September 2-7, 2001.

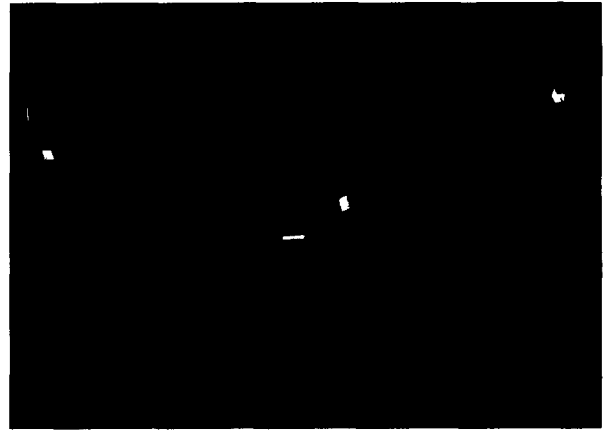


Figure 1: Schematic of the Formation Flying Virtual Structure Space Telescope

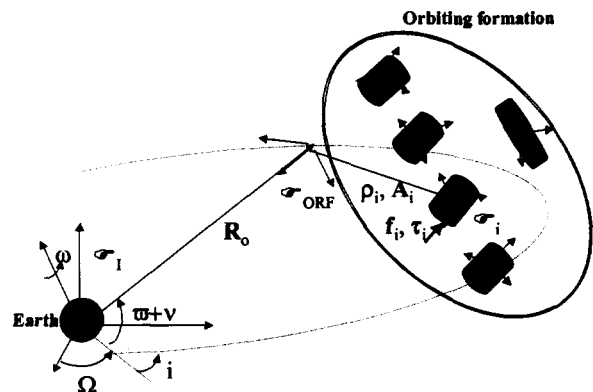


Figure 2. Geometrical Description of Orbiting Formation.

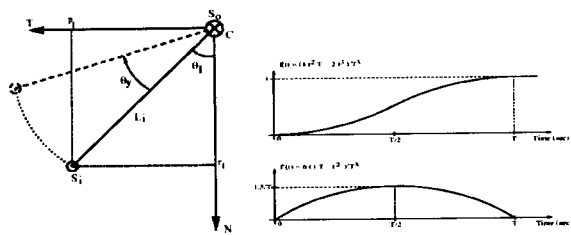


Figure 3. Depiction of Planned Retargeting Slew in orbital plane (left) with commanded profile (right).

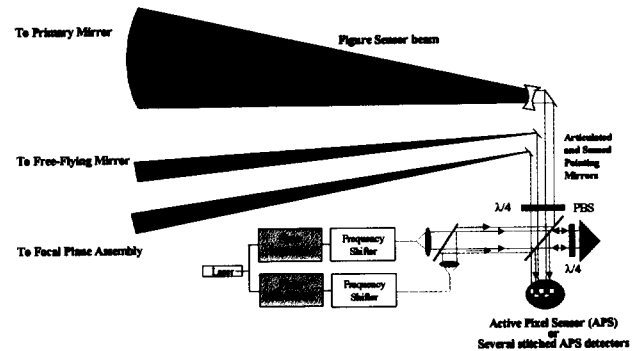


Figure 6. GEOTEL Vector Metrology Sensor

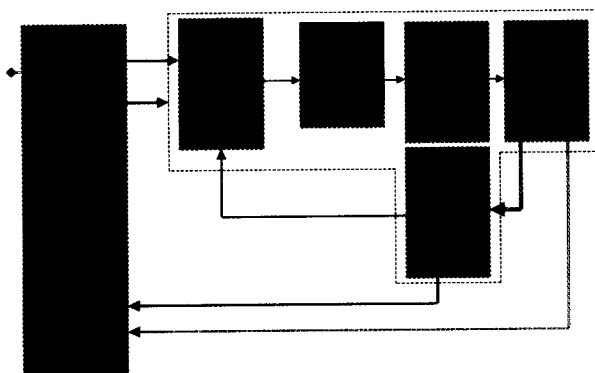


Figure 4. Simulation Architecture

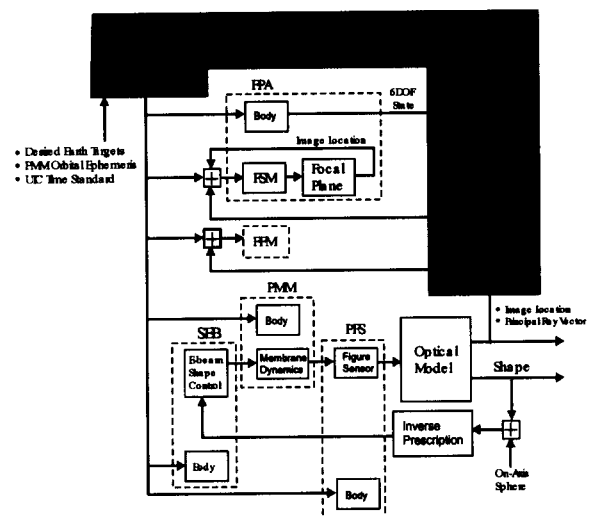


Figure 7. GEOTEL Formation Command & Control Functional Diagram.

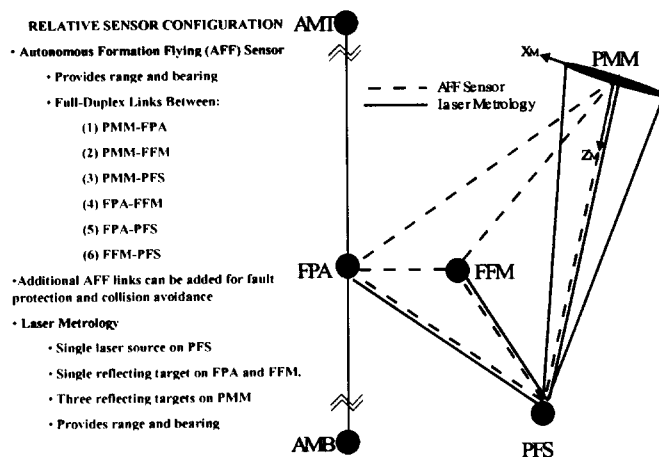


Figure 5. GEOTEL Metrology in a Tethered FPA optional configuration (AMT/AMB along Local Vertical)

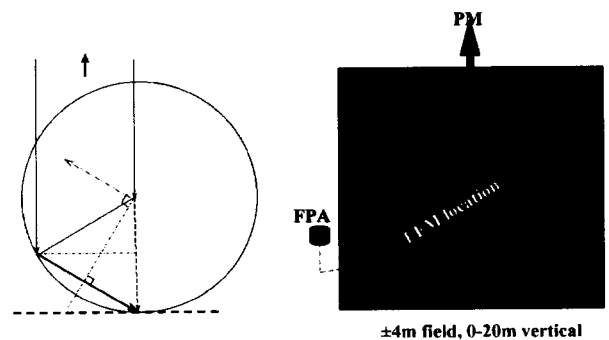


Figure 8. Free-flying Mirror Commander

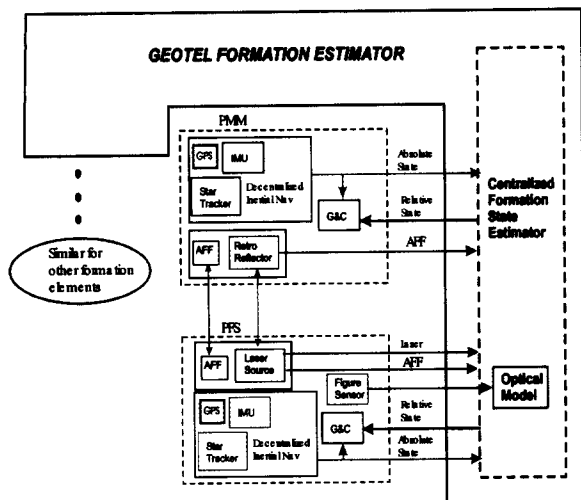


Figure 9. GEOTEL Formation Estimator

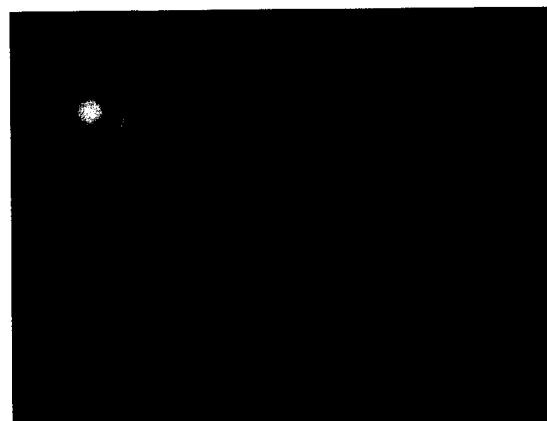


Figure 11. An envisioned application of the GEOTEL concept for exo-solar system planet imaging

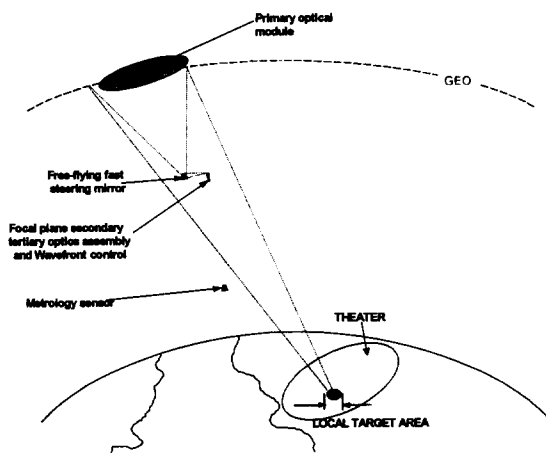


Figure 10. Methodology of Operation of GEOTEL when Imaging a Target on Earth's surface.

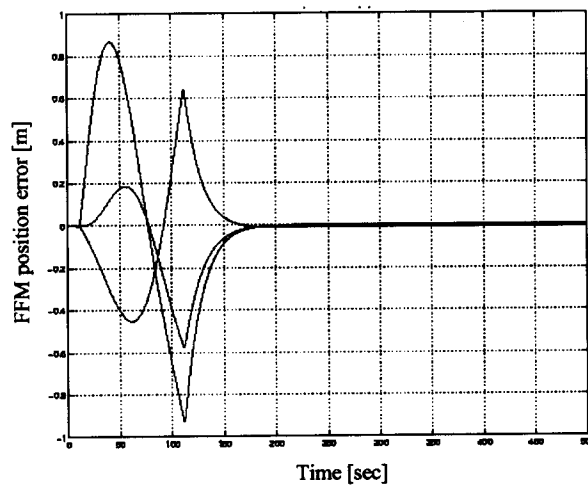


Figure 12. FFM Position Error in meters vs. time during a 1 degree Retargeting in the orbital plane.